Table V. Optimal Geometrical Data for the Various CH_3CO_2 States under Discussion and Corresponding Energies Estimated from the Calculated Curves of Figures 3 and 4

| state	OCO (deg)	CC (Å)	E(est full CI) (hartree)
$1\,^2A''$	112	1.5	−227.6365
$^2A'$	135	1.60	−227.619
$2\,^2A''$	122	≈1.57	−227.619

state	relative energies (eV)
$1\,^2A''$	0.0
$^2A'$	0.476 (10.9 kcal)
$2\,^2A''$	0.476 (10.9 kcal)

several kcal/mol, and are likely to place the $^2A'$ state somewhat too high compared with the $1\,^2A''$.

5. Observations on RCO_2 Behavior (PSS and DDM)

Experimental results which will be reported in detail elsewhere show a remarkable concordance with these calculations, perhaps a concordance which is unique at present, but which holds promise of a future in which theory and experiment will be intimate and specific companion methods for examination of chemical dynamics.

The two methods employed for generating RCO_2 radical (R = Me, Et, *i*-Pr, or *t*-Bu) are:

method I: $RCO_2 Br + Br\cdot \rightarrow Br_2 + RCO_2$

method II: $RCO_2 Br + R'\cdot \rightarrow R'Br + RCO_2$
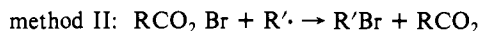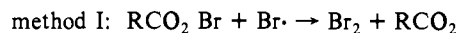
These methods differ in that method II is more exothermic than I by an amount equal to the bond energy difference between Br_2 and R'Br, 21.7 kcal/mol if R' is a primary or secondary alkyl radical. If excited states lie within this energy gap, it is resonable to anticipate[1] that methods I and II will populate different RCO_2 states.

If studied in thermal chain reactions having I or II integral to the chain steps, both of these methods produce H-abstracting radicals showing selectivities for abstractions from primary or secondary C–H bonds with early transition state character. These selectivities are nonetheless different from one another and thus require two H abstractors. In competition with these H-abstraction reactions is the well-known loss of CO_2, leading to R· and ultimately RBr (the Hunsdiecker reaction).

These competition processes were discerned readily at temperatures between −63 and −100 °C. Remarkably, the loss of CO_2 (method I or II) occurs with higher activation energies than the H abstractions, accounting for the earlier failures to recognize chemistry other than the loss of CO_2, since those studies were carried out at room temperature or above. A second unexpected feature of these observations is that *t*-$BuCO_2$ decarboxylates less rapidly by a factor of 10 than $EtCO_2$, the difference in rate being caused by the ∼1 kcal/mol larger E_{act} for loss of CO_2 from the former radical.

These facts are neatly consistent with the rationalization provided by Figures 5 and 6. The decarboxylating RCO_2 is $^2A'$. Steric hindrance to opening the OCO angle from 120 to 140° places the potential energy curve for *t*-$BuCO_2$ higher than that for $EtCO_2$. By analogy with the earlier empirically based assignments,[1] the H abstractor of method I is the $2\,^2A''$, and the H abstractor of method II is the $1\,^2A'$.

6. Summary

In conclusion the present calculations point out the close analogy between the formyl and acetyl radicals despite their difference in nuclear symmetry. It is expected that this analogy can also be carried over to still large carboxylate radicals. The calculations show three low-lying electronic states in these systems whose potential energy minima are separated by probably less than 10 kcal; consideration of vibrational effects might easily reduce this energy gap further. The states show different characteristics with respect to OCO angle variation with the fully symmetric state preferring the large-angle structure (135–140°). In CH_3CO_2 this state is also characterized by a very shallow CC potential well, which should favor CO_2 cleavage; both $^2A''$ states exhibit a deeper CC potential minimum. These calculations are in full accord with the experimental observations in low-temperature radical chain reactions which recognize from kinetic evidence RCO_2's which have two low-lying H-abstracting states, each of which has an energy barrier to loss of CO_2.

Electron-Exchange Processes by Organic Solids: An Electrochemical Solid-State Study of a Series of TTF Radical–Cation Halides with Various Stoichiometries

Myriam Lamache,* Hubert Menet,† and Alec Moradpour‡

Contribution from the Laboratoire de Chimie Analytique, Université Pierre et Marie Curie, 75005 Paris, France, and the Laboratoire de Physique des Solides, Université Paris-Sud, 91405—Orsay, France. Received October 5, 1981

Abstract: The electrochemistry of TTF has been studied in various aqueous media by using carbon paste electrodes. In 1 M acetate, the oxidation of solid TTF proceeds, as in solution, in two one-electron steps, through the successive formation of TTF^+ and TTF^{2+} species. But, in chloride and bromide media, the formation of several mixed-valence salts $((TTF)Cl_{0.7}$, $(TTF)Br_{0.05}$, and $(TTF)Br_{0.7})$ is detected on the current–voltage curves. These studies may provide a new way to investigate the preparative conditions, the compositions and stabilities of various possible solid phases, and the redox behavior of these organic materials.

One-dimensional highly conducting solids, intensively studied over the last decade,[1–4] are presently the subject of renewed interest due to the recent discovery of the existence of superconductivity for some of these organic materials.[5,6]   Various molecular

---

†Laboratoire de Chimie Analytique.
‡Laboratoire de Physique des Solides.

(1) "Chemistry and Physics of One-dimensional metals", Keller, H. J. Ed.; Plenum Press: New York, 1977.

Electron Exchange by Organic Solids

J. Am. Chem. Soc., Vol. 104, No. 17, 1982 4521

properties of the constituents have been examined in the past to look for possible correlations with the desired physical properties. Thus, conductivity values of the extensively studied TTF–TCNQ type (tetrathiafulvalene–tetracyanoquinodimethane) charge-transfer complexes have been correlated with the solution redox potential of the parent electron donors (TTF) and electron acceptors (TCNQ).[7] The consideration of these criteria, though very useful, remains speculative,[8] and it is interesting to obtain new experimental insights closer to the electrochemical "solid-state" properties. This aspect has only recently been illustrated in very interesting studies on the behavior of TTF–TCNQ used as an electrode material in aqueous media.[9–11] Another possible approach, not yet investigated with organic conductors, is provided by the carbon paste electrode analysis, which could readily yield results not accessible by the technique mentioned above.[12]

This electrode, first developed by Schultz and Kuwana[13] and French[14] has been successfully applied to the quantitative electrochemical analysis of sparingly soluble electroactive compounds, mainly sulfide ores[15,16] and metal oxides[17] and also to ferrocene[18] in aqueous media, where this compound is highly insoluble. The paste consists of a mixture of powdered graphite, the electroactive compound, and a pasting liquid ("binder"). Though the exact nature of the electron-exchange processes (direct oxidation or reduction of solid particles or redox reactions involving nevertheless weakly dissolved species[19,20]) is not always easy to establish, the current–voltage curves, recorded at very low potential scan rates (i.e., 10^{-4} V s^{-1}) and for very small amounts of incorporated materials (1 mg), usually correspond to the complete oxidation and/or reduction of the compounds.[18] Under these conditions, the voltammograms obtained for reversible redox systems are comparable to those observed in thin-layer electrochemistry.[21] They exhibit symmetric anodic and cathodic peaks, with the peak current usually occurring at the standard potential of the redox system. For higher scan rates or large amounts of material, the peaks may be distorted because of the ohmic drop,[22] but the half sum $(E_{pa} + E_{pc})/2$ of the anodic (E_{pa}) and cathodic (E_{pc}) peak potentials remains unchanged and equals the standard potential of the redox couple. This technique has enabled the quantitative characterization and investigation of the occurrence of stable redox intermediates formed during the overall transformations of the solid lattices for several inorganic materials. Thus, a series of nonstoichiometric copper compounds has been observed during
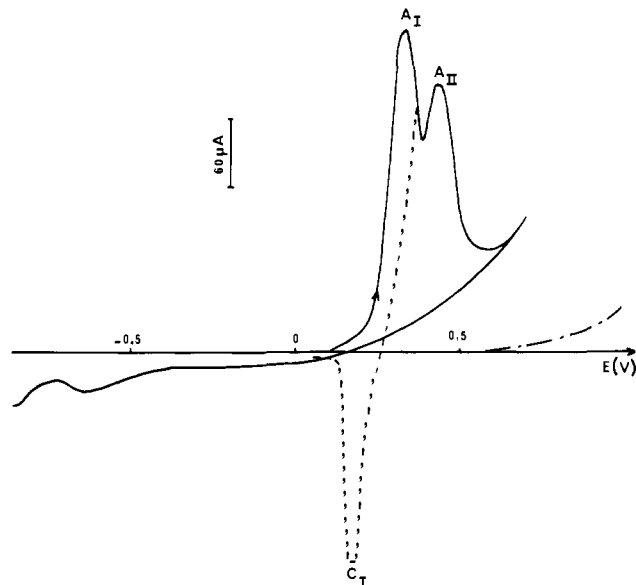

Figure 1. Voltammogram obtained with TTF (2.15 mg) included in a carbon paste electrode containing 1 M sodium acetate and 50 mg of graphite (scan rate 2.5×10^{-5} V s^{-1}); (—·—) residual current without TTF.

the oxidation of cuprous to cupric sulfide.[23] Such studies may also be of interest in the field of solid organic open-shell radical ions because they could provide quantitative information about the existence, the "solid-state" properties, the stabilities of solid phases with various stoichiometries, and, hopefully, some insight into the mechanisms of electron-exchange reactions by these solid particles.

We report in this paper results obtained by using carbon paste electrodes with the well-known series of TTF salts[24] as a first possible example along these lines.

Experimental Section

Electrodes. The carbon paste is obtained by mixing a weighed quantity of electroactive compound (0.2–2 mg of TTF or TTF salt) with a known amount of graphite powder (50 mg) (Johnson-Matthey, nonpelletable quality). An electrolyte (40 μL of 1 M sodium acetate, potassium chloride, or potassium bromide) is added and mixed until the carbon appears uniformly wetted. Electrodes are made by packing the carbon paste into a tube, against a carbon contact, and covering the paste with a glass frit.[18] Such electrodes are used in a stationary mode and are renewed for each determination.

The auxiliary electrode (a platinum wire), the reference electrode (a saturated calomel electrode), and the carbon paste electrode are immersed in an electrochemical cell coontaining the same electrolyte as that used for the paste binder.

Instrumentation. A conventional potentiostat (Tacussel PRT 20-10 X) driven by a signal generator (Tacussel Model GSTP) is used for the voltammetric studies. Cyclic voltammograms are obtained with anodic or cathodic scans starting from the rest potential of the electrode. All potentials are reported vs. the saturated calomel electrode.

Chemicals. The TTF is purchased from Fluka Chemicals. The TTF salts ((TTF)Cl$_{0.7}$ and (TTF)Br$_{0.7}$) are synthesized by electrocrystallization.[25,26]

Results and Discussion

Voltammograms of TTF are strongly dependent on the nature of the supporting electrolyte. The same behavior has already been emphasized by Bard and co-workers,[9–11] who used compressed disks of TTF–graphite (1:1 by weight) and have rationalized the

(2) "Molecular Metals"; Hatfield, W. E., Ed.; Plenum Press: New York, 1979.

(3) Torrance, J. B. *Acc. Chem. Res.* **1979**, *12*, 79.

(4) Khidekel, M. L.; Zhilyaeva, E. I. *Synth. Met.* **1981**, *4*, 1.

(5) Jerome, D.; Mazaud, A.; Ribault, M.; Bechgaard, K. *J. Phys. Lett.*, (*Orasy, Fr.*) **1980**, *41*, L-95.

(6) Bechgaard, K.; Carneiro, K.; Rasmussen, F. B.; Olsen, M.; Jacobsen, C. S.; Pedersen, H. J.; Scott, J. C. *J. Am. Chem. Soc.* **1981**, *103*, 2440.

(7) Wheland, R. C. *J. Am. Chem. Soc.* **1976**, *98*, 3926.

(8) Engler, E. M.; Kaufman, F. B.; Green, D. C.; Klots, C. E.; Compton, R. N. *J. Am. Chem. Soc.* **1975**, *97*, 2921.

(9) Jaeger, C. D.; Bard, A. J. *J. Am. Chem. Soc.* **1979**, *101*, 1690.

(10) Wallace, W. L.; Jaeger, C. D.; Bard, A. J. *J. Am. Chem. Soc.* **1979**, *101*, 4840.

(11) Jaeger, C. D.; Bard, A. J. *J. Am. Chem. Soc.* **1980**, *102*, 5435.

(12) Bauer, D.; Gaillochet, Ph. *Electrochim. Acta* **1974**, *19*, 597.

(13) Schultz, F. A.; Kuwana, T. *J. Electroanal. Chem. Interfacial Electrochem.* **1968**, *10*, 95.

(14) Kuwana, T.; French, W. G. *Anal. Chem.* **1964**, *36*, 241.

(15) Lamache, M.; Bauer, D. *Anal. Chem.* **1979**, *51*, 1320.

(16) Lamache, M.; Kende, D.; Bauer, D. *Nouv. J. Chim.* **1977**, *1*, 377.

(17) Chouaib, F.; Cauquil, O.; Lamache, M. *Electrochim. Acta* **1981**, *26*, 325.

(18) Lamache, M. *Electrochim. Acta* **1979**, *24*, 79.

(19) Laviron, E. *J. Electroanal. Chem. Interfacial Electrochem.* **1978**, *90*, 33.

(20) Lamache, M.; Bauer, D. *J. Electroanal. Chem. Interfacial Electrochem.* **1977**, *79*, 359.

(21) Hubbard, A. T.; Anson, F. C. *Electroanal. Chem.* **1970**, *4*, p 129.

(22) Due to the total electrochemical transformation of the compound incorporated in the carbon paste electrode, the order of magnitude of resulting currents (0.2–1. mA) is much higher than those involved in other standard electrochemical techniques (usually 1–10 μA). This fact accounts for the observed ohmic drops and peak deformation (vide infra, Figure 2).

(23) Brage, M. C.; Lamache, M.; Bauer, D. *Electrochim. Acta* **1979**, *24*, 25.

(24) Scott, B. A.; La Placa, S. J.; Torrance, J. B.; Silverman, B. D.; Welber, B. *J. Am. Chem. Soc.* **1977**, *99*, 6631 and references cited therein.

(25) Kathirganathan, P.; Mucklejohn, S. A.; Rosseinsky, D. R. *J. Chem. Soc., Chem. Commun.* **1980**, 86.

(26) Detailed procedure will be published elsewhere: Lamache, M.; Menet, H.; Weyl, C., in preparation.
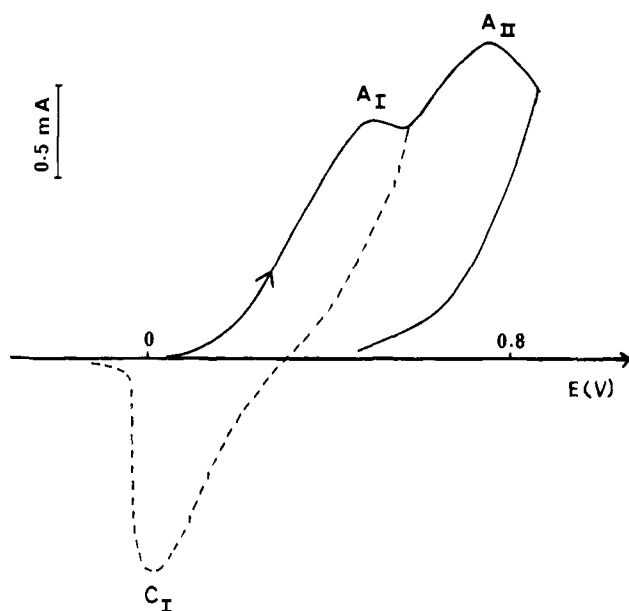
Figure 2. Cyclic voltammogram of TTF (1 mg) in 1 M sodium acetate; scan rate 10^{-3} V s^{-1}.

observed differences as a function of the aqueous solubilities of various organic salts formed with the electrolyte ions. Here again, two quite different behaviors are found, illustrating two different possible situations: (1) TTF$^+$ X$^-$ is soluble (X$^-$ = acetate) and (2) TTF$^+$ X$^-$ is insoluble (X$^-$ = chloride or bromide).

Presently, due to low amounts of materials and to low scan rates, well-defined peaks are obtained for every redox transformation, and moreover, a new interesting behavior related to the occurrence of various nonstoichiometric insoluble species is observed in chloride and bromide media.

Sodium Acetate. A typical cyclic voltammogram of TTF in 1 M acetate is shown in Figure 1. Two peaks, A$_I$ and A$_{II}$, corresponding to peak potentials E_{pA_I} = +0.34 V and $E_{pA_{II}}$ = 0.44, V, are observed when the applied potential is scanned in the positive direction at a rate of 2.5 × 10^{-5} V s^{-1}. Measurement of the total area under the curve indicates a two-electron transfer; though A$_I$ and A$_{II}$ are poorly resolved, it is possible to deduce that each electrochemical reaction corresponds to the exchange of one electron.

When the potential is reversed just after peak A$_I$, a cathodic peak C$_I$, whose area is equivalent to A$_I$, is observed at a peak potential E_{pC_I} = +0.16 V. For higher sweep rates (i.e., 10^{-3} V s^{-1}), E_{pA_I} is shifted anodically and E_{pC_I} cathodically. Thus, if the scan rate is equal to 10^{-3} V s^{-1} (Figure 2), the voltammogram is highly distorted,[22] but the half sum $(E_{pAI} + E_{pCI})/2$ remains unchanged (+0.25 V). This value corresponds to the standard potential of the TTF/TTF$^+$ couple in water and can be compared with the analogous value (+0.33 V) found in acetonitrile.[9,27]

If the potential is reversed after the peak A$_{II}$, no reversible cathodic peak is found, but several ill-defined peaks are observed between −0.4 and −0.8 V (Figure 1). In addition, the measured anodic currents, at potentials more positive than those of A$_{II}$, are clearly higher than those of the expected residual currents without TTF. This indicates a further chemical evolution of the TTF$^+$ oxidation product (TTF^{2+}), which is unstable in aqueous medium.[27] Another hypothesis[28] would be that TTF^{2+}, possibly soluble to a certain extent, may diffuse from the electrode into the solution

(27) Coffen, D. L.; Chambers, J. Q.; Williams, D. R.; Garett, P. E.; Canfield, N. D. *J. Am. Chem. Soc.* **1971**, *93*, 2258.

(28) We acknowledge a reviewer for the suggestion of this possibility.

(29) It is noteworthy that the difference between the standard potentials $E°$ ((TTF)Cl$_{0.7}$/(TTF)Cl) and $E°$ (TTF/(TTF)Cl$_{0.7}$) $(\Delta E°$ = +0.30 *V*) is very close to the calculated electrostatic binding energy gained upon formation of TTF Cl$_\rho$ near the same composition range $(\rho$ = 0.75).[24,30]

(30) Torrance, J. B.; Silverman, B. D. *Phys. Rev. B: Condens. Matter* **1977**, *15*, 788.
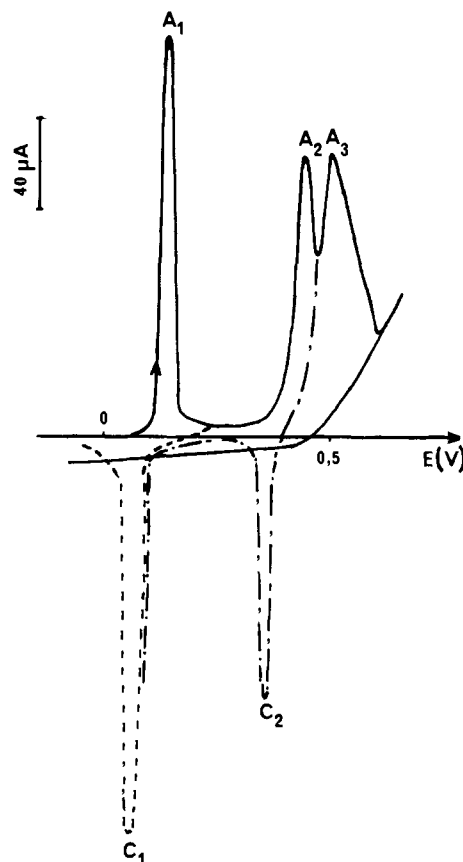
Figure 3. Cyclic voltammogram of TTF (0.85 mg) in 1 M KCl (graphite 50 mg; scan rate 2.5 × 10^{-5} V s^{-1}: a (—); b (—·—); c (---).

Table I. Number of Electrons Exchanged Per TTF Molecule for the Three Anodic Peaks A$_1$, A$_2$, and A$_3$ observed in 1 M KCl as a Function of the Potential Scan Rate (TTF 1 mg; Graphite 50 mg)

pot. scan rate, V s^{-1}	no. of electrons involved in the EC processes			
	A$_1$	A$_2$	A$_3$	A$_1$ + A$_2$ + A$_3$
2.5 × 10^{-5}	0.70	0.30	1	2.0
5 × 10^{-5}	0.66	0.26	1	1.92
10^{-4}	0.24	0.07	0.44	0.75
10^{-3}	0.25	0.25		0.50

and may thus be lost; however, this hypothesis does not account for the observation of the series of cathodic peaks between −0.4 and −0.8 V obtained on the reversed scan in this medium. These results show that in 1 M sodium acetate TTF is oxidized, as usually observed in solution, in two successive one-electron steps through the intermediate formation of soluble TTF$^+$ species; the first oxidation is reversible, while the second one is irreversible even at high sweep rates (Figure 2). The overall process can be written as

$$\text{TTF} \underset{C_I}{\overset{A_I}{\rightleftharpoons}} \text{TTF}^+ \overset{A_{II}}{\longrightarrow} \text{TTF}^{2+} \rightarrow \text{products}$$
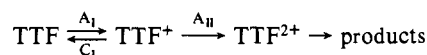
The cathodic peaks observed in the −0.4- to −0.8-V region may be tentatively assigned to the reduction of the not yet identified TTF^{2+} dication byproducts.

Potassium Chloride. The electrochemical behavior of TTF is markedly different in 1 M KCl from that in 1 M NaOAc: three anodic peaks (A$_1$, A$_2$, and A$_3$) are found in potassium chloride (Figure 3). The determination of the total area under the curve indicates a complete electrochemical transformation of TTF for low scan rates (v < 5 × 10^{-5} V s^{-1}) corresponding to the exchange of 2 electrons per TTF molecule (Table I). At 2.5 × 10^{-5} V s^{-1}, the peak potentials are +0.14 V (E_{pA_1}), +0.44 V (E_{pA_2}), and +0.51 V (E_{pA_3}). The peak areas correspond respectively to the exchange

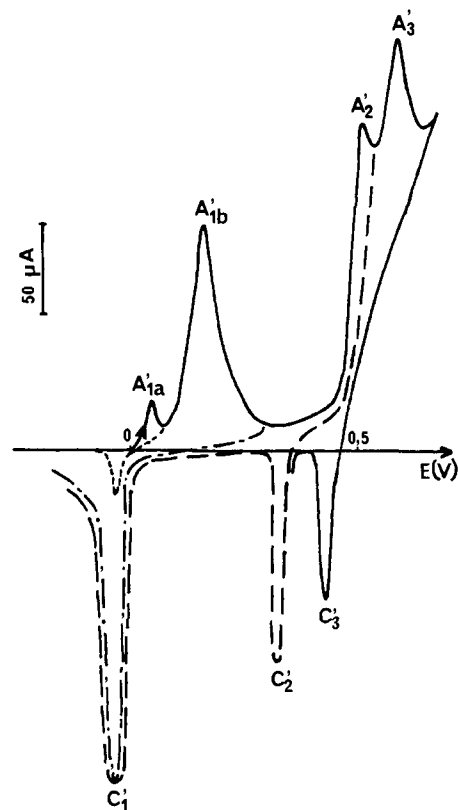*Electron Exchange by Organic Solids*

J. Am. Chem. Soc., Vol. 104, No. 17, 1982 4523
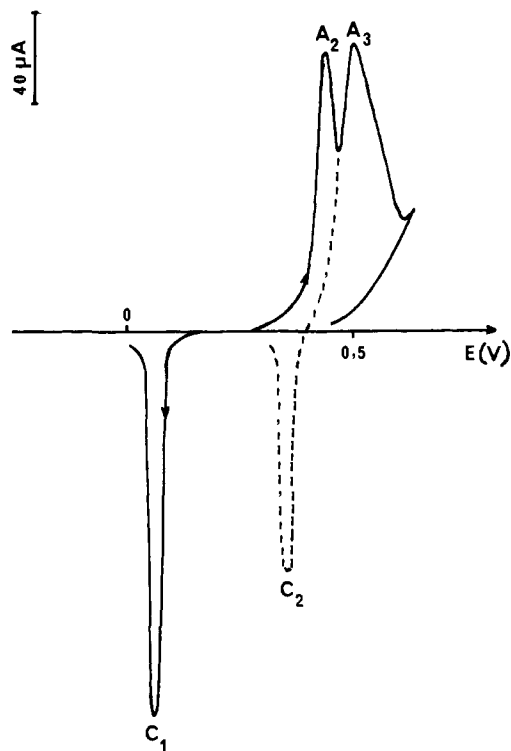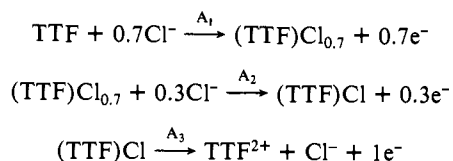

Figure 4. Voltammogram of $(TTF)Cl_{0.7}$ (0.95 mg) in 1 M KCl (graphite 50 mg; scan rate 2.5×10^{-5} V s^{-1}). Anodic peaks A_2 and A_3 as well as cathodic peaks C_1 and C_2 are similar to those of Figure 2.

of 0.7, 0.3, and 1.0 electron per TTF molecule, and these values remain unchanged if the initial amount of TTF introduced in the electrode is varied from 0.5 to 2 mg. If the anodic scan is reversed toward a negative direction after A_1, a cathodic peak C_1 (E_{pC_1} = +0.06 V) with the same area as A_1 is found (Figure 3, curve c). If the cathodic scan starts from A_2 a set of two peaks appears: C_2 (E_{pC_2} = +0.36 V, involving an exchange of 0.3 electron as A_2) and C_1 (Figure 3 curve b). As above, no reversible reduction peak is found for A_3 (Figure 3, curve a), indicating a marked instability of the corresponding oxidation products. As usual, voltammograms obtained at higher scan rates are distorted; thus, at 10^{-3} V s^{-1}, the resolution of A_2 and A_3 has almost vanished (Table I).

In order to assign unambiguously these peaks, carbon paste electrodes containing authentic $(TTF)Cl_{0.7}$ samples, synthesized[26] independently by electrocrystallization, have also been studied. The corresponding voltammograms are shown in Figure 4. The value of the rest potential of the electrode (+0.35 V) is located between the peaks A_1 and A_2 seen previously. On anodic scan, peaks A_2 (0.3 electron) and A_3 (1 electron) are found again. If the first scan is cathodic, C_1 (0.7 electron) is observed, and subsequent scans show also the presence of the cathodic peak C_2 (E_{pC_2} = +0.36 V) corresponding to A_2.
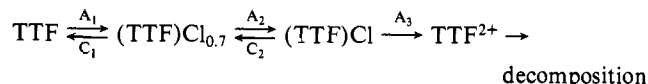
These observations show that the oxidation of TTF in KCl occurs via the formation of insoluble $(TTF)Cl_{0.7}$. The oxidation product of $(TTF)Cl_{0.7}$ is not the soluble TTF^+ species previously formed in 1 M acetate, since the potential of A_3 is different from the oxidation potential of TTF^+ to TTF^{2+} in the latter medium (Figure 3). In KCl, $(TTF)Cl_{0.7}$ is oxidized to insoluble $(TTF)Cl$. The subsequent oxidation of $(TTF)Cl$ leads to some unstable or possibly soluble[28] species (probably TTF^{2+}) since no reversible cathodic peak is found for A_3.

The three anodic peaks may then be ascribed to the following reactions:

$$TTF + 0.7Cl^- \xrightarrow{A_1} (TTF)Cl_{0.7} + 0.7e^-$$

$$(TTF)Cl_{0.7} + 0.3Cl^- \xrightarrow{A_2} (TTF)Cl + 0.3e^-$$

$$(TTF)Cl \xrightarrow{A_3} TTF^{2+} + Cl^- + 1e^-$$

Figure 5. Voltammogram of TTF (1.28 mg) in 1 M KBr (graphite 50 mg; scan rate 2.5×10^{-5} V s^{-1}).

Taking into account the reversibility of some of the electrochemical reactions, we can also summarize the overall process by the following scheme:

$$TTF \underset{C_1}{\overset{A_1}{\rightleftarrows}} (TTF)Cl_{0.7} \underset{C_2}{\overset{A_2}{\rightleftarrows}} (TTF)Cl \xrightarrow{A_3} TTF^{2+} \rightarrow$$

decomposition

From the measured peak potentials E_{pA_1}, E_{pC_1} and E_{pA_2}, E_{pC_2}, it is possible to determine the standard potentials of the TTF/ $(TTF)Cl_{0.7}$ (E° = +0.10 V) and $(TTF)Cl_{0.7}/(TTF)Cl$ (E° = +0.40 V) couples.[29]

Potassium Bromide. The behavior of TTF in 1 M KBr is reminiscent of that previously observed in 1 M KCl, except for the presence of an additional anodic peak. The voltammogram shows four anodic peaks, A_{1a}' (+0.04 V), A_{1b}' (+0.16 V), A_2' (+0.51 V), and A_3' (+0.58 V), corresponding respectively to the exchange of 0.045, 0.65, 0.3, and 1 electron per TTF molecule (Figure 5). On reversed-potential scan, a single cathode peak C_1' (−0.04 V) is found for both anodic peaks A_{1a}' and A_{1b}'; if the potential is reversed after A_2', the curve shows a reversible cathodic peak C_2' (+0.32 V) with an area equal to A_2'. Finally, a small cathodic peak, C_3', is found to correspond to A_3' (Figure 5).

In Figure 6 is shown the voltammogram of $(TTF)Br_{0.7}$ prepared independently by electrocrystallization.[26] Two peaks, A_2' (+0.51 V) and A_3' (+0.58 V), corresponding to 0.3 and 1 electron are observed on anodic scan, and one peak, C_1' (−0.04 V, 0.7 electron), on cathodic scan. On the other hand, the voltammogram of TTFBr, prepd. chemically (by addition of bromide to a solution of TTF^+ in acetonitrile), shows one peak analogous to A_3' at +0.58 V on anodic scan and two peaks at the potentials of C_2' and C_1' on cathodic scan.
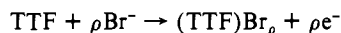
In order to determine the nature of the reaction that takes place at the potential of the first anodic peak A_{1a}', only observed in KBr medium, we have studied the influence of (i) the amount of the TTF introduced in the electrode and (ii) the concentration of the supporting electrolyte (KBr) on the current voltage curves.

The areas of A_{1a}' and A_{1b}' remain unchanged when the amounts of TTF are varied from 0.2 to 5 mg and when the KBr concen-
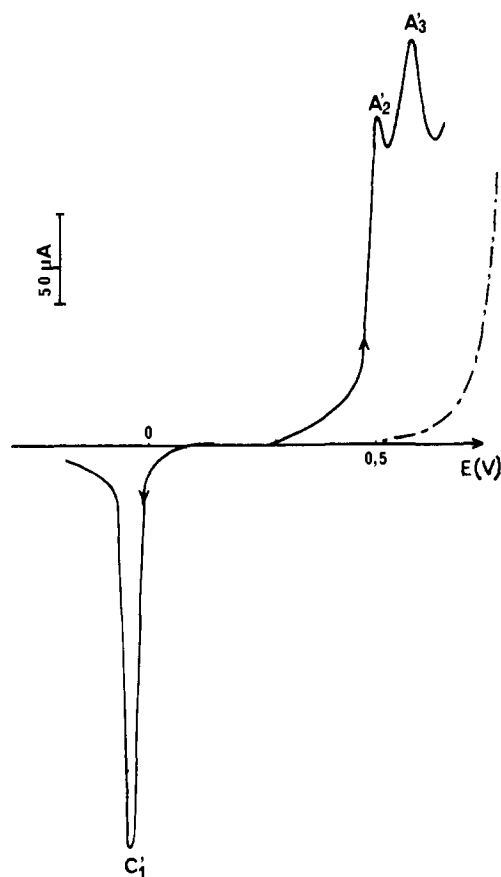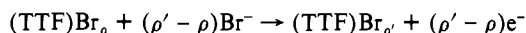
Figure 6. Voltammogram of (TTF)Br$_{0.7}$ (1.45 mg) in 1 M KBr (graphite 50 mg; scan rate 2.5×10^{-5} V s^{-1}). (–·–) Residual current without (TTF)Br$_{0.7}$.

tration is increased from 0.1 to 1 M; at the same time, the values of $E_{pA_{1a}}'$ and $E_{pA_{1b}}'$ become more positive as the bromide concentration decreases and plots of the peak potentials vs. log (Br$^-$) exhibit (–60 mV) slopes. These results suggest that the reactions occurring at the potential of A_{1a}' or A_{1b}' correspond to the formation of two different bromide salts: (TTF)Br$_\rho$ and (TTF)Br$_{\rho'}$ according to

$$\text{TTF} + \rho\text{Br}^- \rightarrow (\text{TTF})\text{Br}_\rho + \rho\text{e}^-$$

and

$$(\text{TTF})\text{Br}_\rho + (\rho' - \rho)\text{Br}^- \rightarrow (\text{TTF})\text{Br}_{\rho'} + (\rho' - \rho)\text{e}^-$$
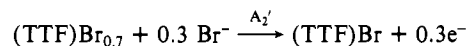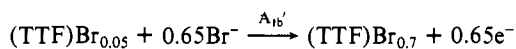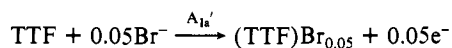
Average values of ρ and ρ' have been determined from the areas of A_{1a}' and A_{1b}' obtained with various amounts of TTF: $\rho = 0.046 \pm 0.004$ (peak A_{1a}') and $\rho' = 0.690 \pm 0.011$ (peaks A_{1a}' and A_{1b}').

As a matter of fact, among the TTF bromides, those near the compositions $\rho = 0.59$ and $\rho = 0.76$ have been isolated,[24] though presently only one nonstoichiometric bromide is detected electrochemically in this ρ range. Bromides whose composition would correspond to $\rho = 0.05$ have never been observed. Our present attempts to isolate this compound have been unsuccessful, but we feel that our voltammetric results are clearly in favor of the formation of this compound.

The oxidation of TTF in the presence of bromide may then be summarized by the following reactions:

$$\text{TTF} + 0.05\text{Br}^- \xrightarrow{A_{1a}'} (\text{TTF})\text{Br}_{0.05} + 0.05\text{e}^-$$

$$(\text{TTF})\text{Br}_{0.05} + 0.65\text{Br}^- \xrightarrow{A_{1b}'} (\text{TTF})\text{Br}_{0.7} + 0.65\text{e}^-$$

$$(\text{TTF})\text{Br}_{0.7} + 0.3 \text{ Br}^- \xrightarrow{A_2'} (\text{TTF})\text{Br} + 0.3\text{e}^-$$

Oxidation of (TTF)Br at more anodic potentials (peak A_3') probably leads to the formation of (TTF)Br$_2$, which is apparently more stable than its chloride analogue, as shown by the existence of a reduction peak, C_3' (Figure 5).

Conclusion

Carbon paste electrodes can be easily and valuably used for the study of the electrochemical behavior of solid organic materials. Such studies have been carried out on a series of TTF salts as a possible example. We have characterized by this technique some previously known nonstoichiometric compounds in this series. The probable formation of a new TTF bromide salt ((TTF)Br$_{0.05}$) with an unusual composition has also been observed.

Clearly, one result of these studies is an interesting way to investigate stable intermediate phases that may occur during the redox transformations of organic solids and to determine the potential regions where these materials are electrochemically inactive and could be used as electrodes.

Further work is, however, required on an extended series of organic material to discuss more precisely the mechanism of the electron-transfer steps of these processes and to achieve rational correlations of the electrochemical behavior investigated with other solid-state physical properties.

An E and C Modification of the $\beta-\pi^*$ Solvation Approach

Peter E. Doan and Russell S. Drago*

Contribution from the School of Chemical Sciences, University of Illinois, Urbana, Illinois 61801. Received November 16, 1981

Abstract: The specific and nonspecific interactions between a solute and polar solvent are treated by an extension of the E and C equation to incorporate nonspecific solvation. An equation of the general form $\Delta X = E_A^* E_B + C_A^* C_B + SD^*$ is offered where ΔX is the observable, E^* and C^* are parameters for the specific donor–acceptor interaction, and S and D^* are solute and solvent parameters for the nonspecific solvation interaction. The treatment is compared to the Kamlet–Taft $\beta-\pi^*$ approach. Similarities and some very significant differences are discussed, indicating the limitations of a $\beta-\pi^*$ analysis. The fundamental cause of the limitations reported for $\Delta\nu_{OH}-\Delta H$ correlations of alcohols is discussed and the correlations are shown to be more general than some reports indicate. The analysis presented lends support to the Kamlet–Taft interpretation of the meaning of $b\beta$, dramatically increases the E and C data base and provides support for the solvation minimized nature of the original E and C data base.

Introduction

The influence of solvent variation on the properties of molecules and reactions has fascinated chemists for a long time. Work from

this laboratory has served to illustrate the significant point that coordinate-bond formation and nonspecific solvation are two independent solvent properties.[1,2] Though considerable success has